RNA (1998), *4*:268–275. Cambridge University Press. Printed in the USA.

Experimental evolution of complexity: In vitro emergence of intermolecular ribozyme interactions

MARTIN M. HANCZYC[1] and ROBERT L. DORIT[2]

[1]Department of Genetics, Yale University, New Haven, Connecticut 06510, USA
[2]Department of Ecology and Evolutionary Biology, Yale University, New Haven, Connecticut 06511, USA

ABSTRACT

In the course of evolving variants of the *Tetrahymena thermophila* Group I ribozyme for improved DNA cleavage in vitro, we witnessed the unexpected emergence of a derived molecular species, capable of acting as a partner for the ribozyme, but no longer autocatalytic. This new RNA species exhibits a deletion in the catalytic core and participates in a productive intermolecular interaction with an active ribozyme, thus insuring its survival in the population. These novel RNA molecules have evolved a precise catalytic interaction with the Group I ribozyme and depend for their survival on the continued presence of active catalysts. This interaction hints at the complexity that may inevitably arise even in simple evolving systems.

Keywords: catalytic RNA; in vitro selection; nucleic acids; self-organization

INTRODUCTION

In vitro molecular systems that incorporate the fundamental features of a Darwinian process have shed considerable light on the catalytic and structural versatility of nucleic acids, proteins, and small organic molecules (Tuerk & Gold, 1990; Beaudry & Joyce, 1992; Ellington & Szostak, 1992; Green & Szostak, 1992; Bartel & Szostak, 1993; Lehman & Joyce, 1993a; Hirao & Ellington, 1995; Wright & Joyce, 1997). By focusing not only on the desired endpoints of selection, but on the trajectory, replicability, and dynamics of the evolving molecular population, in vitro systems also provide a window onto the evolutionary process. This emphasis on the evolutionary constraints guiding the emergence of novel molecular species characterized some of the early work in experimental evolution (Kramer et al., 1974; Eigen, 1987). Recent work has once again focused on the evolutionary uses and implications of in vitro evolution model systems (Lehman & Joyce, 1993b; Ekland et al., 1995; Wlotzka & McCaskill, 1997).

We report here on the evolution of complexity in a system originally designed to evolve Group I ribozyme derivatives showing enhanced cleavage of a specific DNA target sequence (Beaudry & Joyce, 1992; Tsang & Joyce, 1994, 1996). We have witnessed the unexpected development of a stable class of noncatalytic molecules, descended from the *Tetrahymena thermophila* catalytic Group I ribozyme, and dependent upon active ribozymes for survival in the population. This new molecular species now coexists alongside the evolving catalysts. Our initial homogeneous population of autonomous molecules has thus given rise to multiple molecular species involved in novel and more complex intermolecular interactions.

RESULTS AND DISCUSSION

The experimental system capitalizes on the ability of a modified derivative of the *Tetrahymena thermophila* Group I intron (L-21) to cleave an exogenous substrate. In our experiments, a short DNA oligonucleotide anneals to a complementary internal guide sequence of the L-21 ribozyme, thus forming a mimic of the P1 stem (Herschlag & Cech, 1990). The catalytic activity of this ribozyme is initiated by positioning of this P1 stem within the catalytic core (Michel & Westhof, 1990), and by subsequent nucleophilic attack on the corresponding 5′ splice site of the P1 stem by the 3′-most G (G414) of the L-21 ribozyme. This coordinated cleavage–ligation reaction results in the covalent attachment of the 3′ moiety of the cleaved substrate to G414, yielding a “tagged” ribozyme (Zaug

Reprint requests to: Robert L. Dorit, Department of Ecology and Evolutionary Biology, Yale University, 165 Prospect Street, New Haven, Connecticut 06511, USA; e-mail: rdorit@beagle.biology.yale.edu.

& Cech, 1986). Subsequent reverse transcription and amplification steps are dependent on the presence of the tag (Fig. 1A; Beaudry & Joyce, 1992).

An initial population of 10^{13} L-21 molecules, evolving with a constant mutation rate of 0.1%/position/generation, was selected over five generations for improved cleavage of a DNA target oligonucleotide. The characterization of this evolving population included the random cloning of a sample of individual ribozyme molecules. Forty-seven such clones were subsequently sequenced in their entirety. These ribozyme sequences included an evolved family of slightly shortened variants, which we term Δ8/7 molecules. Thirty of the 47 sequenced molecules (64%) were members of this family and exhibited deletions of 12 or more contiguous nucleotides in the catalytic core, characteristically occurring between the P8 and P7 stems. These deletions obliterate the junction between P8 and P7 (J8/7, see Fig. 2) and likely disrupt the structure of the canonical Group I catalytic core.

One representative of this Δ8/7 family, clone G5C, was selected for further analysis; its sequence is shown in Figure 2. This molecule exhibits the characteristic 12-bp deletion within the catalytic core (positions 298–309), as well as two additional single-nucleotide changes (A370 → U; A373 → U) that may disrupt the formation of the lower half of the P9.2 stem. When tested for catalytic activity, G5C showed no detectable DNA cleavage or tag ligation. Other members of the Δ8/7 family were also tested and they too showed no catalytic activity. They include G5B (Δ298–309; U56 → C); G5O (Δ298–312); G5AK (Δ298–309; Δ150; U71 → A; A184 → G); G5AR (Δ298–309; U176 → C); G5AT (Δ298–309; U49 → C; U287 → C); G5BF (Δ298–309; A153 → G); G5BM (Δ298–309; G58 → A).

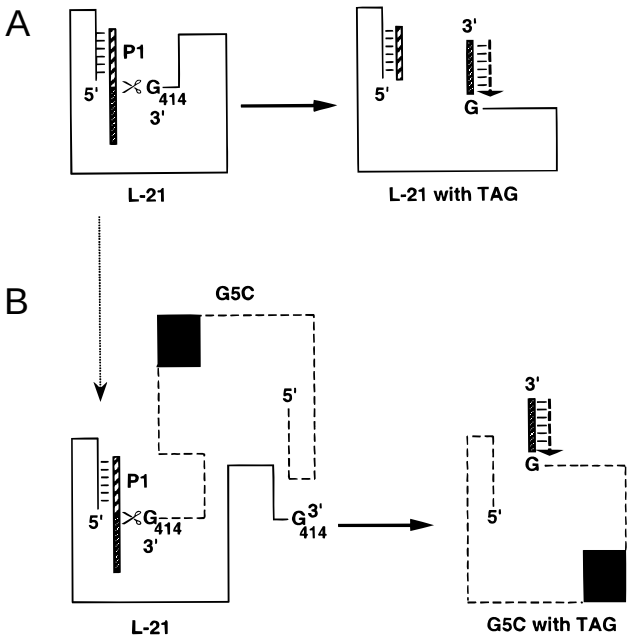

FIGURE 1. Proposed model for intra- and intermolecular tagging. **A:** Intramolecular tagging of the L-21 ribozyme. Shaded bar represents the DNA substrate oligonucleotide. Pairing between the substrate and the 5′ region of the L-21 ribozyme forms the P1 stem. Scissors indicate the site of nucleophilic attack by G414 on the bound substrate. Following cleavage, the 3′ moiety of the cleaved oligonucleotide is covalently linked to the 3′ end of the ribozyme (tagging). Dashed arrow paired to the tag sequence represents the oligomer used to prime cDNA synthesis from the tagged molecules. **B:** Proposed intermolecular interaction between L-21 and G5C. The L-21 ribozyme is represented as a solid line. G5C is shown as a dashed line, with the black box indicating the deletion in the catalytic core. The substrate oligonucleotide and the nucleophilic attack are represented as described in A. As depicted, these reactions result in the tagging of both L-21 and G5C.

Given that ribozyme molecules are specifically selected in our evolution in vitro system for their ability to cleave and ligate the tag sequence, how can we account for the persistence of noncatalytic Δ8/7 molecules in our experiments? Activity assays using a mixture of the catalytically active L-21 ribozyme and G5C (Fig. 3, lanes 1–6) reveal that the shortened derivative has become an intermolecular partner for the L-21 ribozyme. As a result of this interaction, G5C acquires the tag sequence necessary to insure its survival into the next generation. Other representatives of the catalytically inactive Δ8/7 family can also successfully serve as partners in the tagging reaction (data not shown).

To understand how the intermolecular interaction between L-21 and G5C results in the tagging of both molecular species (Fig. 3), we focused our attention on the two key components of the catalytic reaction: the nucleophilic G414 and its target, the P1 substrate complex. The tagging of both the catalytic and partner RNA molecules must result from nucleophilic attack by their respective terminal G414 residues. Two mechanisms could account for the presence of a tag on G5C. The first would involve a nucleophilic attack by G5C on the bound substrate forming the P1 stem of either L-21 or G5C. Alternatively, a nucleophilic attack by G5C on the already tagged L-21 would result in the transfer of the tag from the 3′ end of L-21 to the 3′ end of G5C. We explored this latter mechanism by using sodium periodate to oxidize the nucleophilic G414 hydroxyl groups of both L-21 and G5C. As shown in Figure 4, this chemical modification of L-21 results in a complete loss of self-tagging activity (lanes 3–4). A mix containing oxidized L-21 and unmodified G5C, however, still shows tagging of G5C (lanes 7–8). The tagging of L-21 is thus not a precondition for G5C tagging. Under these conditions, the oxidized L-21 is acting purely as a catalyst mediating the interaction between the P1 substrate complex and the partner molecule.

The target of nucleophilic attack was directly examined by modifying the 5′ ends of both the L-21 and G5C molecules. We designed a short PCR amplimer that resulted in truncated ribozymes that lack the first five nu-

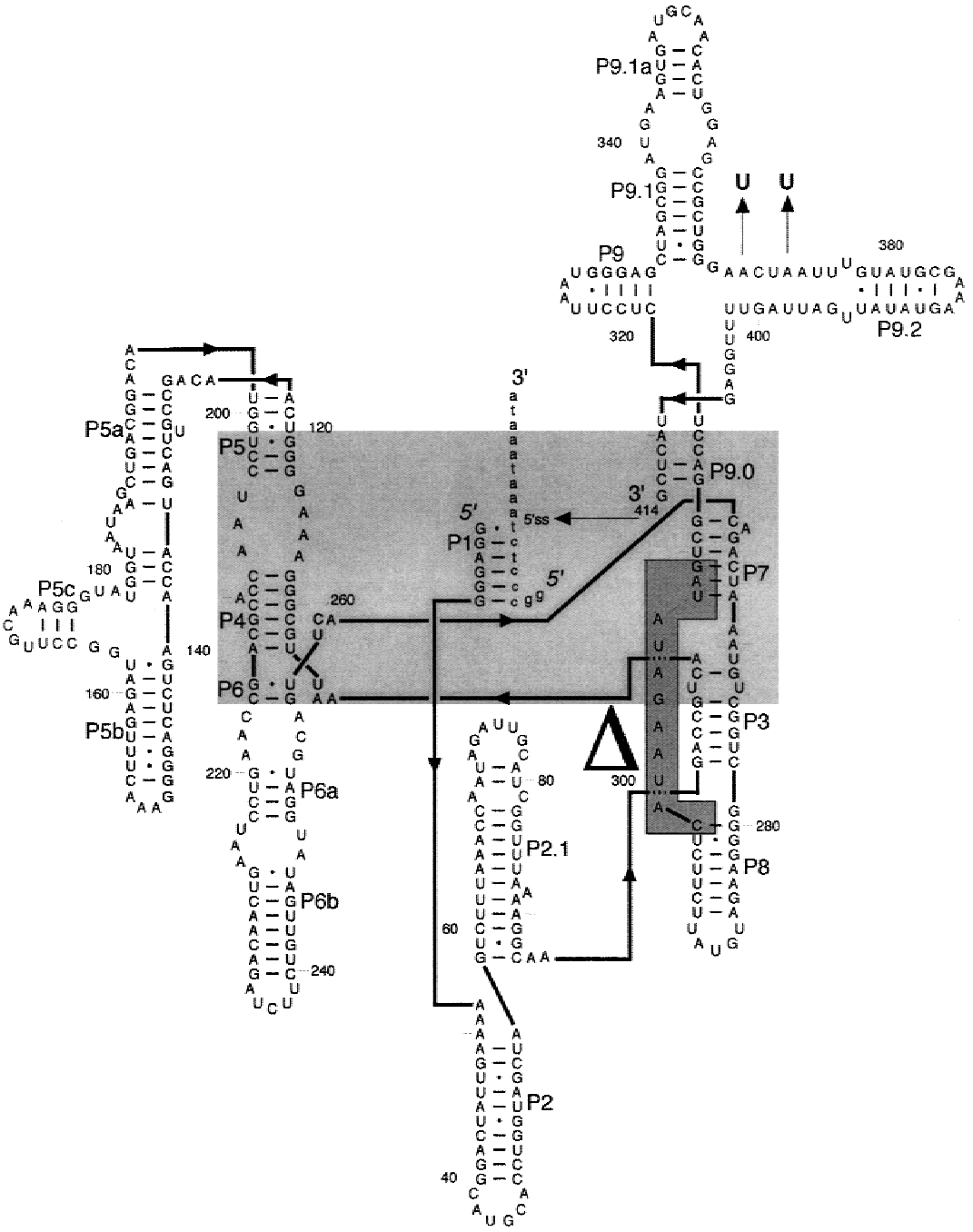

FIGURE 2. Changes characterizing clone G5C, superimposed on the secondary structure model of L-21 ribozyme (Cech et al., 1994). Lightly shaded area encompasses the conserved catalytic core. Heavily shaded box shows the 12-nt deletion in G5C. The two A → U nucleotide substitutions occur in the P9.2 region; the lower half of the P9.2 stem is shown unpaired as a consequence of these nucleotide changes. DNA substrate bound to the ribozyme is shown in lower case. The site of nucleophilic attack by G414 on the 5′ splice site is indicated as **5′ss**.

cleotides. This truncation eliminates the pairing between the RNA molecule and the substrate DNA oligonucleotide, and thus prevents the formation of a P1 stem. A mixture containing intact L-21 and truncated G5C still results in the tagging of both molecules (Fig. 5, lanes 11–12). The converse experiment, using intact G5C and truncated L-21, does not yield tagged molecules (Fig. 5, lanes 9–10). Thus, under our experimental conditions, it is the P1 of the intact, catalytically active ribozyme (L-21) that acts as the target of the nucleophilic attack and is the source of the tag for both L-21 and G5C. Based on the above experiments, we depict a possible mechanism for the intermolecular interaction between L-21 and G5C in Figure 1B.

Can all catalytically inactive molecules arising in our in vitro system be tagged by the original L-21 ribo-

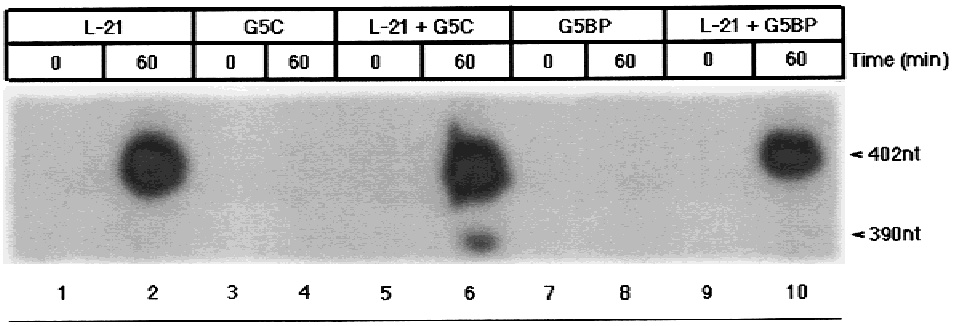

FIGURE 3. Tagging of the active L-21 ribozyme and of its potential partners, G5C and G5BP. Gel-purified RNA molecules were incubated with labeled DNA oligonucleotide substrate. Three-microliter aliquots were withdrawn at 0 and 60 min and resolved on a 3.5% acrylamide, 8 M urea gel. Lanes 1 and 2, 1 pmol of L-21 was used in the reaction represented; lanes 3 and 4, 9 pmol G5C; lanes 5 and 6, 1 pmol L-21 and 9 pmol G5C; lanes 7 and 8, 9 pmol G5BP; lanes 9 and 10, 1 pmol L-21 and 9 pmol G5BP. Upper band at 402 nt represents tagged L-21; lower band at 390 is tagged G5C.

zyme? We examined members of the Δ8/7 family that arise as the result of the mutational background in our experiment but do not survive the selection step. One example of such a transient molecule, G5BP, was detected in the sequencing survey of generation 5 (see Materials and Methods). The sequence of G5BP closely resembles G5C, displaying the characteristic 12-nt Δ8/7 deletion (positions 298–309) in the catalytic core, but lacking the two additional nucleotide changes (positions 370 and 373) present in G5C. As shown in Figure 3, the G5BP variant is not autocatalytic (lanes 7–8), and, in contrast with G5C, is not tagged by the L-21 ribozyme (lanes 9–10). This result indicates that the presence of the 12-nt deletion alone does not insure a successful intermolecular interaction. Although disruption of the catalytic core appears to inactivate L-21 derivatives, it does not automatically give rise to an intermolecular partner that can be successfully tagged by the remaining active ribozymes. In the case of G5C and other members of the Δ8/7 family, additional nucleotide changes have specifically evolved in conjunction with the deletion, enabling the productive interaction between active ribozyme and its inactivated descendants.

What are the relative efficiencies of the successful intra-and intermolecular catalytic reactions? We investigated the kinetics of tag incorporation over time in populations containing only L-21 or a 9:1 mixture of G5C and L-21. The results (Fig. 6) reveal that the presence of a ninefold excess of the noncatalytic partners (G5C) does not significantly affect the autocatalytic performance of the active (L-21) ribozymes. In comparison, G5C tag incorporation proceeds approximately one order of magnitude less efficiently, as indicated by the slopes of the reaction curves in Figure 6B, obtained by regression over the linear portion of the curves. These curves suggest that a significant number of both catalyst and partner molecules will be tagged under the in vitro selection conditions in our experiments.

As noted previously, the Δ8/7 family of molecules comprises a significant proportion of our evolving population. The lower rate of tag incorporation for members of the Δ8/7 family is presumably offset by their relative advantage in the replication steps within each generation of in vitro evolution, possibly due to their shorter length or to changes in their secondary or tertiary structure. We examined the possible replicative advantage of G5C over L-21 in the PCR amplification

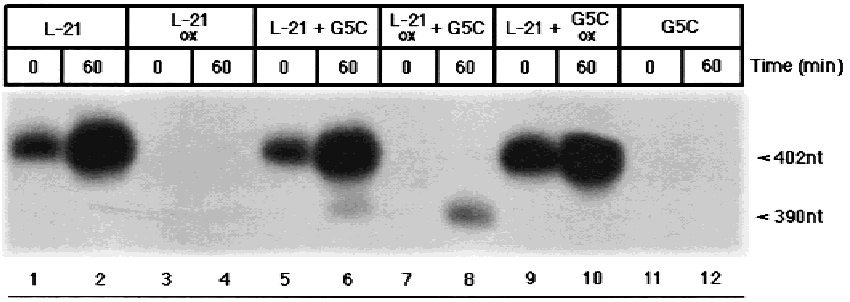

FIGURE 4. Tagging of RNA molecules before and after oxidation of nucleophile G414. The notation "**ox**" indicates that the particular RNA molecule was oxidized with NaIO4. Lanes 1 and 2, 1 pmol of L-21 was used in the reaction represented; lanes 3 and 4, 1 pmol of oxidized L-21; lanes 5 and 6, 1 pmol of L-21 and 9 pmol of G5C; lanes 7 and 8, 1 pmol of oxidized L-21 and 9 pmol of G5C; lanes 9 and 10, 1 pmol L-21 and 9 pmol of oxidized G5C; lanes 11 and 12, 9 pmol of G5C. The band at 402 nt is the tagged L-21 ribozyme; tagged G5C is 390 nt in length.

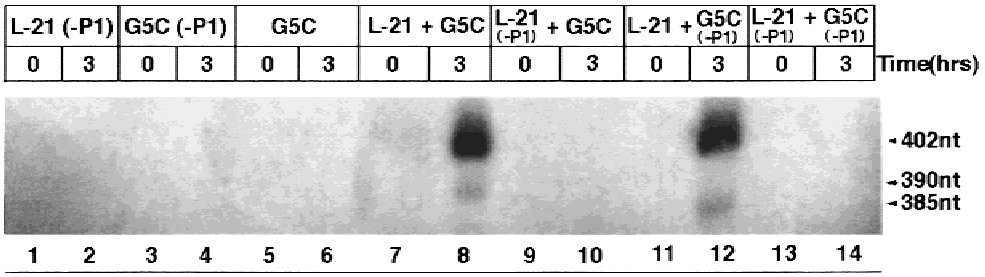

FIGURE 5. Tagging of L-21 and G5C in the presence and absence of P1 stem formation. Full-length ribozymes and truncated RNA molecules (designated **−P1**) lacking the first five nucleotides (22–26) of the internal guide sequence were assayed for cleavage of the DNA oligonucleotide substrate. Lanes 1 and 2, 1 pmol of L-21(-P1) was used in the reaction represented; lanes 3 and 4, 9 pmol G5C(-P1); lanes 5 and 6, 9 pmol G5C; lanes 7 and 8, 1 pmol L-21 and 9 pmol G5C; lanes 9 and 10, 1 pmol L-21(-P1) and 9 pmol G5C; lanes 11 and 12, 1 pmol L-21 and 9 pmol G5C(-P1); lanes 13 and 14, 1 pmol L-21(-P1) and 9 pmol G5C(-P1). The highest band at 402 nt represents tagged L-21, the middle band (390 nt) tagged G5C, and the lowest band (385 nt), tagged G5C(-P1).

step; the results are summarized in Figure 7. The data suggest that G5C has a twofold or greater (2.1–6-fold) replicative advantage over L-21 over a broad range of initial template ratios. This replicative advantage in the PCR step alone may account for the persistence of the Δ8/7 molecules despite their lower rate of tagging. We suspect that the Δ8/7 molecules may gain additional advantage in the other transcription and amplification steps of the protocol.

Although the long-term stability of the molecular partnership we describe is unknown, members of the Δ8/7 deletion family were first observed in the third generation of our experiment (1 of 19 clones), and increase in frequency in subsequent generations (30 of 47 clones after generation 5). Dynamical arguments suggest that cooperative interactions between the evolving species must be occurring if the system is to remain stable (Hofbauer & Sigmund, 1988). In vivo counterparts to

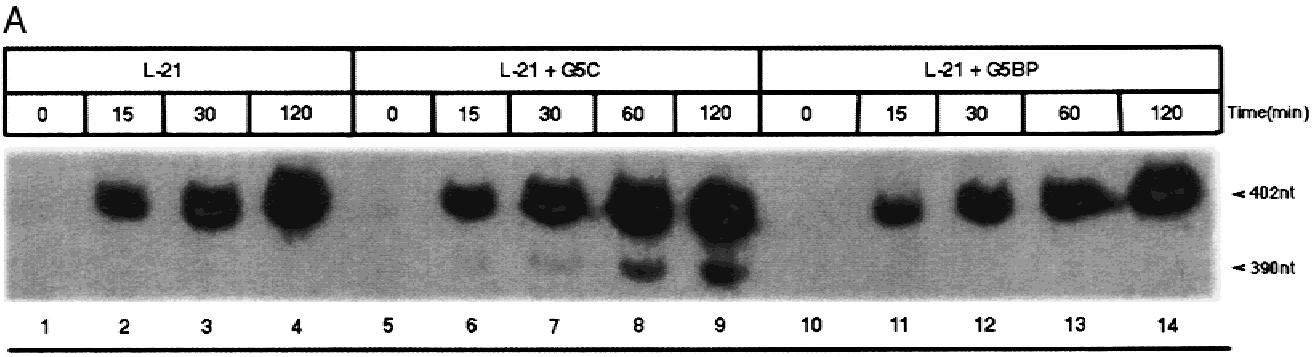

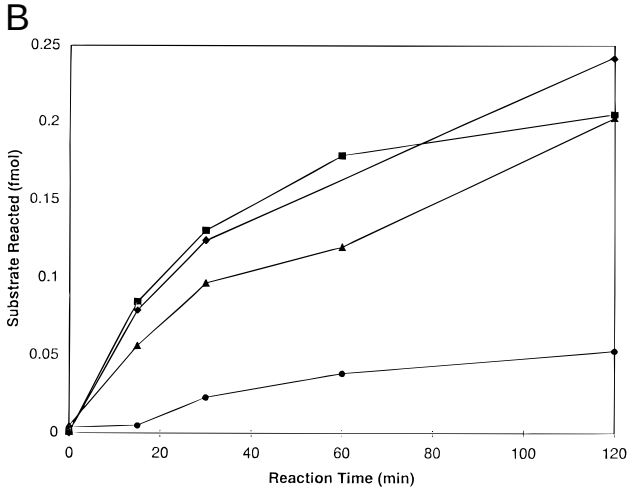

FIGURE 6. Kinetics of the intra- and intermolecular tagging reaction. Gel-purified RNA molecules were incubated in the presence of labeled DNA oligonucleotide substrate; 3-μL aliquots were withdrawn from this reaction at 0, 15, 30, 60, and 120 min and resolved on a 3.5% acrylamide, 8 M urea denaturing gel. Kinetic rates were obtained by regression through the linear portion of the k_{obs} data. **A:** RNA concentrations are as follows: 1 pmol L-21 (lanes 1–4); 1 pmol L-21 and 9 pmol G5C (lanes 5–9); 1 pmol L-21 and 9 pmol G5BP (lanes 10–14). **B:** Graph displays the amount of labeled oligonucleotide substrate incorporated into tagged molecules as a function of reaction time; slopes were calculated in fmol of substrate incorporated per minute. Labeling of L-21 alone (♦, k_{obs}: 4.17×10^{-3} fmol/min); labeling of L-21 (■, k_{obs}: 4.30×10^{-3} fmol/min) and G5C (●, k_{obs}: 0.98×10^{-3} fmol/min), respectively, in a reaction mixture represented in lanes 5–9; labeling of L-21 (▲, k_{obs}: 3.06×10^{-3} fmol/min) in a reaction mixture containing both L-21 and G5BP (lanes 10–14).

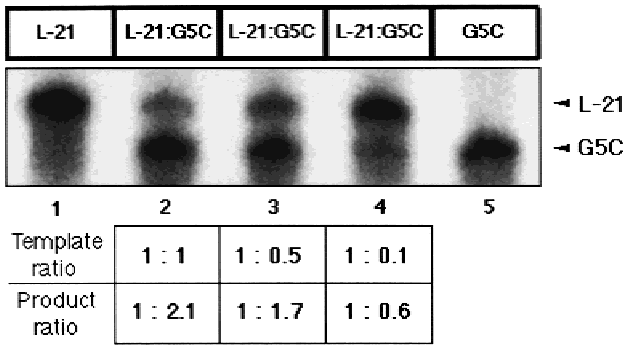

FIGURE 7. Comparative PCR amplification of L-21 and G5C. PCR amplification reactions were prepared using either a single starting template (L-21 or G5C) or mixtures containing varying ratios of L-21 and G5C templates. Lanes 1 and 5 show the amplification products obtained from 20 fmol of L-21 and G5C templates, respectively. Lanes 2, 3, and 4 show the amplification resulting from various starting ratios of L-21 to G5C templates. Each reaction contains a total of 20 fmol of starting template. Template ratios of 1:1, 1:0.5, and 1:0.1 refer to the initial proportions of L-21 and G5C, respectively. Product ratios represent the proportion of L-21 and G5C, respectively, present after PCR amplification, normalized to the product yield of L-21 amplification. In each lane, 1/25 of the completed PCR reactions were resolved and the amounts of amplified product quantified as counts per minute per mm^2 (cpm/mm^2). Upper band represents L-21; lower band represents G5C. Means and standard deviations, derived from five independent trials, are as follows: 1:1 template ratio (L-21: 1,011 ± 175 cpm/mm^2, G5C: 2,109 ± 297 cpm/mm^2); 1:0.5 template ratio (L-21: 5,238 ± 626 cpm/mm^2, G5C: 8,885 ± 2,174 cpm/mm^2); 1:0.1 template ratio (L-21: 3,212 ± 583 cpm/mm^2, G5C: 1,973 ± 327 cpm/mm^2).

the in vitro scenario we describe may include defective interfering virus particles. Such particles arise as spontaneous deletion mutants that are dependent upon the wild-type virus for replication. The success of these defective virus particles may be due in part to their reduced genome length, which results in a more expeditious replication by polymerases (Norkin & Tirrell, 1982; Woodworth-Gutai et al., 1983; Szathmary, 1992; Furuya et al., 1993; Kirkwood & Bangham, 1994; Meyers & Thiel, 1995).

Previous theoretical work dealing with the emergence of biological organization foreshadows a transition from simple to more complex evolving systems (Fontana & Buss, 1994). The presence of the Δ8/7 family, which now forms a significant and persistent part of our in vitro ecosystem, shows a new level of complexity evolving in a relatively simple in vitro scheme despite the absence of direct selection for such complexity. In effect, we have witnessed a transition from a system composed entirely of autonomous ribozymes mediating their own survival to a system in which multiple molecular species interact, ensuring the survival of the newly evolved molecular partners as well as of the active catalysts. Our system capitalizes on a capacity for intermolecular interaction that is clearly latent in the L-21 ribozyme. Although intermolecular reactions between two L-21 ribozymes are never seen under our selection and assay conditions, we are able to detect a low level of productive interaction between L-21 molecules under very permissive reaction conditions. The success of G5C depends on its ability to exploit this intermolecular potential. As a result of the appearance of the Δ8/7 family of molecules, intermolecular interactions emerge as an important component of the dynamics of this system.

The evolution and persistence of noncatalytic molecular partners may set the stage for the generation of further complexity. The molecules of the Δ8/7 family survive in the population because of their interaction with active ribozymes. This interaction frees the evolved partner molecules from the selective constraints imposed by the need to maintain their own catalytic core. They may now be in a position to incorporate novel internal sequences, provided that these do not disrupt the structural elements necessary for the intermolecular partnership. Their replication insured by the interaction with active ribozymes, these partner molecules may be the raw material for the evolution of novel functions. Each novel function may in turn beget further complexity in the form of additional interactions, parasites, and novel molecules, eventually culminating in self-maintaining systems (Fontana & Buss, 1994). The origin of much of the complex RNA-based machinery present in contemporary organisms—ribosomes, spliceosomes, and the like—may well have originated by the gradual buildup of structural and functional complexity analogous to what we have witnessed here.

MATERIALS AND METHODS

Preparation of L-21 ribozymes

L-21 ribozyme was prepared by PCR amplification of plasmid pT7L-21 (courtesy of T. Cech) mediated by an upstream primer (**TAS2.1**) containing a T7 promoter and the first 20 nt (positions 22–41) of the L-21 ribozyme (5′-CTGCAGAATT CTAATACGACTCACTATAGGAGGGAAAAGTTATCAGG-3′) and a downstream primer (**T13**) complementary to the 3′ end of the ribozyme (positions 378–414; 5′-CGAGTACTCCAA AACTAATCAATATACTTTCGCATAC-3′). PCR conditions: 30 cycles at 92 °C, 1 min; 45 °C, 1 min; 72 °C, 1 min in a buffer including 1.5 mM $MgCl_2$. The amplified product (200 ng) was subsequently transcribed using T7 RNA polymerase (NEB). Transcription was allowed to proceed for a minimum of 120 min at 37 °C. Transcription products were resolved on a 5% denaturing acrylamide gel and visualized by UV shadowing. The relevant band was sliced out of the gel, the RNA eluted overnight in a buffer containing 200 mM $NaCl_2$, 10 mM Tris, pH 7.5, and 0.5 mM EDTA, and subsequently recovered by standard ethanol precipitation.

Truncated RNA molecules lacking the first five nucleotides (22–26) of the internal guide sequence were prepared as above, but initial PCR amplification used a shortened 5′ primer (**NOP1**; 5′-CTGCAGAATTCTAATACGACTCACTATAGAAA AGTTATCAGGC-3′).

Periodate oxidation of RNA molecules

RNA molecules (130 pmol) in a 50-μL reaction volume were oxidized with a 50-μL volume of 20 mM $NaIO_4$. The reaction proceeded on ice for 30 min; RNA was then ethanol precipitated, washed, and resuspended under standard conditions (Nadeau et al., 1984).

In vitro selection conditions

The selection experiments were performed following the protocols described in Beaudry and Joyce (1992), with minor modifications. The evolving population contained approximately 10^{13} RNA molecules, with an estimated inherent mutation rate of 0.1%/position/generation, supplying continuous variation to the system. During the cleavage step, the ribozyme population was incubated with a fivefold excess of the DNA oligonucleotide substrate (5×10^{13} substrate molecules). Cleavage and tagging were allowed to proceed at 37 °C for 1 h (generations 1–2); 30 min (generation 3), and 15 min (generations 4–5) in a 20-μL reaction containing a final 10 mM $MgCl_2$ concentration.

Isolation of individual ribozyme variants

The individual molecules characterized in this study were obtained by cloning the PCR amplification products of the heterogeneous ribozyme population undergoing in vitro evolution. PCR products were ligated into T-tailed pBlueScript and individual clones isolated from single colonies and prepared according to standard protocols. The sample examined after five generations of in vitro evolution included (1) active L-21 descendants, (2) successful intermolecular partners (including G5C), and (3) newly-arisen transient molecules (such as G5BP) that would not survive subsequent selection.

Kinetic assays

Kinetic measurements were conducted under the conditions described in the previous section. Gel-purified RNA molecules were incubated at 37 °C in the presence of 50 pmol ^{32}P 3′-labeled DNA oligonucleotide substrate (5′-GGCCC TCTAAATAAATA-3′) in a 20-μL reaction containing 10 mM $MgCl_2$, 30 mM EPPS, pH 7.5. Three-microliter aliquots were withdrawn from this reaction at 0, 15, 30, 60, and 120 min and resolved on a 3.5% acrylamide, 8 M urea denaturing gel. Labeled products, corresponding to tagged RNA molecules, were visualized using a phosphorimager (Fujix BAS 2000) and quantified using the NIH Image package. Analysis was performed on a Macintosh computer using the public domain NIH Image program (developed at the U.S. National Institutes of Health and available at http: //rsb.info.nih.gov/nih-image/). Kinetic rates were obtained by regression through the linear portion of the k_{obs} data.

Ribozyme tagging assays

Gel-purified RNA molecules were incubated with 20 pmol terminal transferase ^{32}P 3′ end-labeled DNA oligonucleotide substrate (5′-GGCCCTCTAAATAAATA-3′) in a 20-μL reaction containing 10 mM $MgCl_2$, 30 mM EPPS, pH 7.5, at 37 C. Three-microliter aliquots were withdrawn at 0 and 60 min and resolved on a 3.5% acrylamide, 8 M urea gel. Results were visualized via phosphorimaging, as described above.

Comparative PCR amplification assay

A constant 20 fmol of plasmid template were amplified via PCR as described previously, with the addition of 2–4 μCi ^{32}P dATP. After 30 cycles of amplification, 1/25 of the reactions (4 μL) was resolved on a 3.5% denaturing acrylamide gel. Labeled products corresponding to amplified PCR DNA were visualized using a phosphorimager (Fujix BAS 2000) and quantified using MacBAS Ver2.0. Five replicates of each template ratio were prepared and subsequently amplified and the mean and standard deviation of the product counts (cpm/mm^2) calculated.

ACKNOWLEDGMENTS

We thank S. Altman, R. Breaker, L. Buss, K. Cole, J. Doudna, J. Huckaby, K. Kidd, J. Kim, N. Maizels, S. Paabo, M. Riley, G. Wagner, A. Weiner, and two anonymous reviewers for their helpful criticism and suggestions, T. Cech for the pT7L plasmid, and G. Joyce for help and guidance with the evolution in vitro system. This work supported by the Yale Science Development Fund and an NSF Doctoral Dissertation Improvement Grant.

Received August 29, 1997; returned for revision October 3, 1997; revised manuscript received December 15, 1997

REFERENCES

Bartel DP, Szostak JW. 1993. Isolation of new ribozymes from a large pool of random sequences. *Science 261*:1411–1418.

Beaudry AA, Joyce GF. 1992. Directed evolution of an RNA enzyme. *Science 257*:635–641.

Cech TR, Damberger SH, Gutell RR. 1994. Representation of the secondary and tertiary structure of group I introns. *Nature Struct Biol 1*:273–280.

Eigen M. 1987. New concepts for dealing with the evolution of nucleic acids. *Cold Spring Harbor Symp Quant Biol 52*:307–20.

Ekland EH, Szostak JW, Bartel DP. 1995. Structurally complex and highly active RNA ligases derived from random RNA sequences. *Science 269*:364–370.

Ellington AD, Szostak JW. 1992. Selection in vitro of single-stranded DNA molecules that fold into specific ligand-binding structures. *Nature 355*:850–852.

Fontana W, Buss LW. 1994. "The arrival of the fittest:" Toward a theory of biological organization. *Bulletin of Mathematical Biology 56*:1–64.

Furuya T, Macnaughton TB, La Monica N, Lai MM. 1993. Natural evolution of coronavirus defective-interfering RNA involves RNA recombination. *Virology 194*:408–413.

Green R, Szostak J. 1992. Selection of a ribozyme that functions as a superior template in a self-copying reaction. *Science 258*:1910–1915.

Herschlag D, Cech TR. 1990. DNA cleavage catalysed by the ribozyme from *Tetrahymena*. *Nature 344*:405–409.

Hirao I, Ellington AD. 1995. Re-creating the RNA world. *Curr Biol 5*:1017–1022.

Hofbauer J, Sigmund K. 1988. *The theory of evolution and dynamical systems*. New York: Cambridge Press.

Kramer FR, Mills DR, Cole PE, Nishihara T, Spiegelman S. 1974. Evolution in vitro: Sequence and phenotype of a mutant RNA resistant to ethidium bromide. *J Mol Biol 89*:719–736.

Kirkwood TB, Bangham CR. 1994. Cycles, chaos, and evolution in virus cultures: A model of defective interfering particles. *Proc Natl Acad Sci USA 91*:8685–8689.

Lehman N, Joyce GF. 1993a. Evolution in vitro of an RNA enzyme with altered metal dependence. *Nature 361*:182–185.

Lehman N, Joyce GF. 1993b. Evolution in vitro: Analysis of a lineage of ribozymes. *Curr Biol 3*:723–734.

Meyers G, Thiel HJ. 1995. Cytopathogenicity of classical swine fever virus caused by defective interfering particles. *J Virol 69*:3683–3689.

Michel F, Westhof E. 1990. Modelling of the three-dimensional architecture of group I catalytic introns based on comparative sequence analysis. *J Mol Biol 216*:585–610.

Nadeau JG, Singleton CK, Kelly GB, Weith HL, Gough GR. 1984. Use of ribonucleosides as protecting groups in synthesis of polynucleotides with phosphorylated terminals. *Biochemistry 23*:6153–6159.

Norkin LC, Tirrell SM. 1982. Emergence of simian virus 40 variants during serial passage of plaque isolates. *J Virol 42*:730–733.

Szathmary E. 1992. Natural selection and dynamical coexistence of defective and complementing virus segments. *J Theor Biol 157*:383–406.

Tsang J, Joyce GF. 1994. Evolutionary optimization of the catalytic properties of a DNA-cleaving ribozyme. *Biochemistry 33*:5966–5973.

Tsang J, Joyce GF. 1996. Specialization of the DNA-cleaving activity of a group I ribozyme through in vitro evolution. *J Mol Biol 262*:31–42.

Tuerk C, Gold L. 1990. Systematic evolution of ligands by exponential enrichment: RNA ligands to bacteriophage T4 DNA polymerase. *Science 249*:505–510.

Wlotzka B, McCaskill JS. 1997. A molecular predator and its prey: Coupled isothermal amplification of nucleic acids. *Chem Biol 4*:25–33.

Woodworth-Gutai M, Celeste A, Sheflin L, Sclair M. 1983. Naturally arising recombinants that are missing portions of the simian virus 40 regulatory region. *Mol Cell Biol 3*:1930–1936.

Zaug AJ, Cech TR. 1986. The intervening sequence RNA of *Tetrahymena* is an enzyme. *Science 231*:470–475.